ISSN: 1999-6691, e-ISSN: 2782-3709 DOI: http://doi.org/10.7242/1999-6691/2025.18.2.14

Research article

Finite element modeling of reduced grain boundaries elasticity in nanocrystalline metals

A. Talakesh[1], ***A. Torabi***[2]

[1] *Department of Mechanical Engineering, University of Isfahan, Isfahan, 81746-73441, Iran*
[2] *Department of Mechanical Engineering, Ferdowsi University of Mashhad, Mashhad, 91775-1111, Iran*

Nanocrystalline metals consist of two distinct phases: the crystalline phase, namely grains, and the intercrystalline phase, which includes grain boundaries, triple junctions, and quadruple nodes. Weakening of elasticity in the intercrystalline phase of nanocrystalline metals, especially in grain boundaries, causes a decrease in the overall elastic modulus. Consequently, studying the elastic behavior and calculating the elasticity of grain boundaries are critical to the understanding of nanocrystalline metals. The purpose of this research is to model the elasticity of grain boundaries in nanocrystalline metals and calculate it. For this purpose, five different metal samples with different crystalline structures are considered. For each sample, three representative volume elements (RVEs) with different grain sizes and constant grain boundary thickness are modeled. The behavior of the crystalline phase is assumed to be elastic with cubic symmetry, while the behavior of grain boundaries is assumed to be elastically isotropic. Uniaxial tension is then simulated using a finite element analysis to calculate the Young's modulus of the RVEs. The weakening coefficient for grain boundaries is obtained through this analysis. To verify the validity of this coefficient, the Young's modulus of the simulated RVEs is compared with the Young's modulus extracted from molecular dynamics simulation and experiments reported in the literature.

Keywords: grain, grain boundary, nanocrystalline metals, representative volume elements, weakening coefficient, Young's modulus

Received: 30.05.2024 / *Published online*: 30.07.2025

1. Introduction

Investigating the behavior of materials is one of the most significant issues in various engineering disciplines, especially in the field of mechanics. Over time, considerable efforts are devoted to achieving deeper comprehension of material behavior. Microscopic investigation of material involves considering materials as crystalline structures, and evaluation of material behavior undertaken through their microstructures [1]. A grouping of crystalline structures that exhibit uniform orientation is referred to as a grain, and the interface between these grains, which leads to their separation, is termed grain boundaries [2]. Nowadays, extensive research is conducted on the microstructure of materials and their crystal structures. It is shown that changes in the behavior and properties of materials are due to changes in their microstructures [3, 4]. The elasticity of grain boundaries is considerably weaker in comparison to grains. The mechanical properties of metals and alloys, particularly at the nanoscale and under microstructural examinations, are profoundly influenced by the size of grains and a constant grain boundary thickness [5, 6]. Hence, in nanocrystalline metals, the grain size exerts a significant influence on the majority of their mechanical properties. Due to the significant effect of grain boundaries on the mechanical properties of crystalline metals, and because studying the microstructure of these metals is critical for understanding and predicting their behavior, investigating the changes in grain boundaries' elastic properties is of considerable importance. In order to design nanocrystalline metals and alloys with optimal and tunable mechanical properties, it is necessary and important to know the dependence of these metals and alloys' properties on their grain size and grain boundary thickness. The ability to quantify the relationship between the dependence of the mechanical properties of metals on their grain sizes and the grain boundary of the microstructure leads to better manufacturing, processing, and improving the mechanical properties. Hence, the main objective of this research is to model grain boundaries in nanocrystalline metals and calculate their elastic properties using FE analysis.

Zheng et al. [7] introduced a relationship based on the strain energy, which is a function of the difference in vacancy concentration between the stressed and stress-free states, the constant coefficient of the geometric factor, the applied stress, and the free space energy with the elastic coefficient of the grain boundary. As an example, they used this method to obtain the elastic properties of the grains of the allotropic polycrystalline alpha-iron. Zhu et al. [8] investigated the effect of surface grain boundary energy and non-local boundary reactions on Young's modulus of copper nanocrystals based on continuum elasticity theory [9, 10]. By combining interfacial energy and grain strain energy, they obtained the effective Young's modulus of grains. By comparison with experimental results, the accuracy of the obtained results was demonstrated. The results of this analysis indicate that with an increase in grain size, the Young's modulus of nanocrystals also increases. Then, they used the law of mixtures and presented the ratio of the representative volume element (RVE) Young's modulus of nanocrystals to the Young's modulus of the crystal alone based solely on the grain size. Yeheskel et al. [11] applied the ultrasonic wave method. The basis of this investigation was the analysis and measurement of the density and velocity of sound waves. It was observed that the low elastic modulus of magnesium nanocrystals was due to the low density and elastic modulus of its boundaries. Therefore, based on the experiments conducted, with a decrease in grain size, the effective elastic modulus also decreased. Kim et al. [12] investigated the elastic properties of a polycrystalline metal based on continuum mechanics theories presented by [13, 14]. This theory elucidated the fourth-order equilibrium equation that related the displacement field and connections in the grain boundaries. They demonstrated the influence of longitudinal scale at the nanoscale, showing that with its increase, the effective Young's modulus decreased and the Poisson's ratio increased. The

rate of change of the elastic modulus and the effective Poisson's ratio decreased with a minimal decrease in the longitudinal scale of the grain boundaries. The FEM (Finite Element Method) was employed to model the elastic coefficients of the grain boundaries and it demonstrated that the size of the elastic modulus of nanocrystalline metals is directly related to the grain size. They examined this result for copper metal with different grain sizes. Xu and Davila [6] investigated the effect of grain size on the elastic properties of nanocrystalline aluminum using the molecular dynamics (MD) method. Simulation results indicated that the elastic properties of nanocrystalline aluminum were non-sensitively correlated with grain size when it exceeded 13 nm. However, for grain sizes smaller than 13 nm, there was a higher sensitivity of the elastic modulus to grain size. Initially, with a reduction in grain size, the elastic modulus also decreased, and, when the grain size reached 9 nm, further reduction in grain size led to a more pronounced decrease in the elastic modulus. Latapie and Farkas [3] investigated the effect of grain size on the elastic properties of the iron nanocrystal. They conducted this investigation through atomic computer simulation and molecular static method. They performed necessary examinations on three RVEs with different grain sizes and constant grain boundary thickness and found that with increasing grain size, the elastic modulus in iron metal increases. Pan et al. [5] investigated the tensile properties of the tantalum nanocrystal using the MD method. In this study, 7 samples with 16 grains were considered. These samples differed only in grain size but had the same grain boundary thickness. These samples were created using a specific algorithm, and their boundary conditions were considered as periodic boundary conditions. By examining the plotted stress-strain diagrams, it was observed that with increasing grain size, the elastic modulus of the RVE also increases. Zhou et al. [15] calculated the Young's modulus of the aluminum nanocrystal and investigated the effects of changes in grain size on the Young's modulus. Sanders et al. [16] assessed copper and palladium nanocrystals, with initial grain sizes ranging from 10 to 110 nm. They performed operations of hardening and softening on these nanocrystals and observed that, as the grain size decreases, the elastic modulus and consequently the hardness of the metal decrease. Softening refers to the reduction in the size of nanocrystal grains, leading to a decrease in the elastic modulus and thus softening of the nanocrystals. Schiotz et al. [17] investigated the effect of grain size on the elastic modulus of the nanocrystalline metal, which leads to softening and hardening of that. They examined the influence of grain size on its elastic modulus. They introduced that, usually, the hardness of the metal decreases with the decrease in grain size. They attributed this to the elastic properties of the grain boundaries, which are generally lower compared to the grains. They achieved this by inducing partial strain and then calculating the Young's modulus of the nanocrystals.

The elasticity of grain boundaries compared to grains is significantly weaker. Reducing the grain size in a fixed grain boundary thickness leads to an increase in the volume fraction effect of grain boundaries. Consequently, this decreases the overall elasticity of nanocrystals, specifically, at grain sizes smaller than 20 nm [15]. In this grain size, the volume fraction effect of the intermediary nanocrystal phase, i.e., triple junctions, and particularly grain boundaries exert a greater influence on the Young's modulus and other elastic properties of nanocrystals. By considering the aforementioned aspects, it is imperative to thoroughly understand the elastic properties and precisely calculate the elasticity of grain boundaries. This is crucial for the development of optimal and enhanced designs. To the best knowledge of researchers, the research conducted in this field focused on investigating the effects of grain size on the elastic modulus of nanocrystalline metals using both theoretical and experimental methods [15, 18–22]. Despite the considerable influence of grain boundary elasticity on the overall properties, a significant gap exists in the research dedicated to its quantifiable calculation. By surpassing these deficiencies and advancing the field, this study aims to fill the existing gap. The objective of this research is to model the elasticity of grain boundaries and calculate their elastic modulus in nanocrystalline metals.

This paper is prepared as follows: the formulation and RVE modeling are described in Sec. 2; the FE simulation is described in Sec. 3; the results are presented in Sec. 4; and the article is concluded in Sec. 5.

2. Method

To model the elasticity of grain boundaries in nanocrystalline metals, three RVEs representing nanocrystals are constructed for five metals with different crystal structures. Each of these RVEs has varying grain sizes and a constant grain boundary thickness. The Young's modulus (elasticity) of grain boundaries is computed through uniaxial tensile simulations. The following assumptions underpin this approach:

– Constitutive Law: Linear elasticity (Hooke's Law);
– Grain Properties: Elastic behavior with cubic symmetry;
– Grain Boundary Properties: Isotropic for the intermediate phase in the RVE;
– Modeling Approach: 3D RVE modeling, FE simulation, and extraction of constitutive property equations.

The summary of the method is described following, and in the subsequent subsections, it will be explained in detail step by step (Fig. 1).

1. Preparation of the RVE through the partitioning method based on the parameters specified for modeling, i.e., the grain boundary thickness to the grain size ratio.

2. Defining the behavioral model of grains and grain boundaries in the RVE. The grain behavior model is represented as the cubic symmetry and implemented through a UMAT subroutine. Grain boundaries are considered isotropic, and their Young's modulus is taken as a coefficient (grain boundary weakening coefficient, α) of the Young's modulus of the RVE.

3. Performing uniaxial tensile simulation through FE software, Abaqus.

4. Determining Young's modulus of the RVE through the uniaxial tensile simulation performed in step 3.

5. Comparison between the Young's modulus obtained from FE simulations and the Young's modulus extracted from MD simulations and experimental tests from other studies.

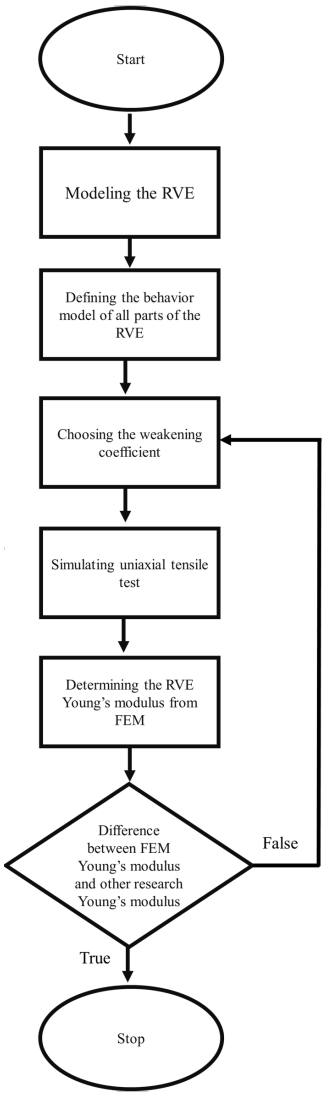

Fig. 1. Weakening coefficient calculation flowchart

6. Presenting the value of the selected weakening coefficient as the case of a difference of less than 1% between Young's modulus values obtained from the FEM and that extracted from other studies. Otherwise, an escalation in the weakening coefficient is envisaged, necessitating a repetition of steps from 3 onwards.

2.1. Formulation

Since the behavior of grains is assumed to be elastic and cubic symmetry, in this section, constitutive equations for materials with cubic symmetry are developed [23, 24]. In other words, these equations are applied to model the relationship between stress and strain quantities of grains in the RVE of nanocrystal; these equations are expressed in this section.

The relationship between stress and strain for materials in an index notation is represented as $\sigma_{ij} = C_{ijkl}E_{kl}$, where C_{ijkl} is a fourth-order tensor [25]. This relationship is expressed in matrix form in two dimensions as follows:

$$\begin{bmatrix} \sigma_{11} \\ \sigma_{22} \\ \sigma_{33} \\ \sigma_{12} \\ \sigma_{13} \\ \sigma_{23} \end{bmatrix} = \begin{bmatrix} C_{1111} & C_{1122} & C_{1133} & C_{1112} & C_{1113} & C_{1123} \\ & C_{2222} & C_{2233} & C_{2212} & C_{2213} & C_{2223} \\ & & C_{3333} & C_{3312} & C_{3313} & C_{3323} \\ & Symm & & C_{1212} & C_{1213} & C_{1223} \\ & & & & C_{1313} & C_{1323} \\ & & & & & C_{2323} \end{bmatrix} \begin{bmatrix} \varepsilon_{11} \\ \varepsilon_{22} \\ \varepsilon_{33} \\ 2\varepsilon_{12} \\ 2\varepsilon_{13} \\ 2\varepsilon_{23} \end{bmatrix}. \quad (1)$$

Eq. (1) can be rewritten in Voigt notation [26] as follows:

$$\begin{bmatrix} \sigma_1 \\ \sigma_2 \\ \sigma_3 \\ \sigma_4 \\ \sigma_5 \\ \sigma_6 \end{bmatrix} = \begin{bmatrix} C_{11} & C_{12} & C_{13} & C_{14} & C_{15} & C_{16} \\ & C_{22} & C_{23} & C_{24} & C_{25} & C_{26} \\ & & C_{33} & C_{34} & C_{35} & C_{36} \\ & Symm & & C_{44} & C_{45} & C_{46} \\ & & & & C_{55} & C_{56} \\ & & & & & C_{66} \end{bmatrix} \begin{bmatrix} \varepsilon_1 \\ \varepsilon_2 \\ \varepsilon_3 \\ 2\varepsilon_4 \\ 2\varepsilon_5 \\ 2\varepsilon_6 \end{bmatrix}. \quad (2)$$

Considering the existing symmetries, Eq. (2) for materials with cubic symmetry is written in the form present in Eq. (3). It should be noted that the engineering constants required for materials with cubic symmetry are three constants: C_{11}, C_{12}, and C_{44}:

$$\begin{bmatrix} \sigma_1 \\ \sigma_2 \\ \sigma_3 \\ \sigma_4 \\ \sigma_5 \\ \sigma_6 \end{bmatrix} = \begin{bmatrix} C_{11} & C_{12} & C_{12} & 0 & 0 & 0 \\ & C_{11} & C_{12} & 0 & 0 & 0 \\ & & C_{11} & 0 & 0 & 0 \\ & Symm & & C_{44} & 0 & 0 \\ & & & & C_{44} & 0 \\ & & & & & C_{44} \end{bmatrix} \begin{bmatrix} \varepsilon_1 \\ \varepsilon_2 \\ \varepsilon_3 \\ 2\varepsilon_4 \\ 2\varepsilon_5 \\ 2\varepsilon_6 \end{bmatrix}. \quad (3)$$

Matrix C_{ij} in Eq. (3) is the stiffness matrix, and its inverse, i.e., S_{ij}, which defines the relationship $\boldsymbol{\varepsilon} = \mathbf{S}\boldsymbol{\sigma}$, is called the compliance matrix. The constants expressed for materials with a cubic symmetry behavior in the compliance matrix are as specified in Eq. (4), and its inverse is written in the form of the matrix in Eq. (5):

$$S = \begin{bmatrix} \frac{1}{E} & \frac{-\nu}{E} & \frac{-\nu}{E} & 0 & 0 & 0 \\ & \frac{1}{E} & \frac{-\nu}{E} & 0 & 0 & 0 \\ & & \frac{1}{E} & 0 & 0 & 0 \\ & Symm & & \frac{1}{\mu} & 0 & 0 \\ & & & & \frac{1}{\mu} & 0 \\ & & & & & \frac{1}{\mu} \end{bmatrix}, \quad (4)$$

$$C=\begin{bmatrix} \frac{E(\nu-1)}{2\nu^2+\nu-1} & \frac{-E\nu}{2\nu^2+\nu-1} & \frac{-E\nu}{2\nu^2+\nu-1} & 0 & 0 & 0 \\ & \frac{E(\nu-1)}{2\nu^2+\nu-1} & \frac{-E\nu}{2\nu^2+\nu-1} & 0 & 0 & 0 \\ & & \frac{E(\nu-1)}{2\nu^2+\nu-1} & 0 & 0 & 0 \\ & Symm & & \mu & 0 & 0 \\ & & & & \mu & 0 \\ & & & & & \mu \end{bmatrix}, \tag{5}$$

where ν is the Poisson ratio, E is the Young's modulus, and μ is the shear modulus.

Each grain inherently has a different and unique orientation; therefore, after developing the constitutive equations for individual grains, which are terminologically called local, it becomes imperative to generalize these equations for the entire RVE of the nanocrystal. Considering the various orientations of each grain, by utilizing these angles and the coordinate axis transformation, it is possible to derive a generalized stiffness matrix for all grains present within the RVE. For this purpose, it is necessary to apply the transformation matrix between two right-handed coordinate systems. Considering $\mathbf{e}_1, \mathbf{e}_2, \mathbf{e}_3$ and $\mathbf{e}_1^{'}, \mathbf{e}_2^{'}, \mathbf{e}_3^{'}$ as the corresponding unit vectors of two right-handed Cartesian coordinate systems, $\mathbf{e}_1, \mathbf{e}_2, \mathbf{e}_3$ can be formed in such a way that they align with $\mathbf{e}_1^{'}, \mathbf{e}_2^{'}, \mathbf{e}_3^{'}$ through a rigid-body rotation or a rotation followed by a reflection about $\mathbf{e}_1^{'}, \mathbf{e}_2^{'}, \mathbf{e}_3^{'}$ [9]. Consequently, the orthogonal tensor $\mathbf{Q}$ relates the two basis vectors $\mathbf{e}_i$ and $\mathbf{e}_i^{'}$ to each other as follows:

$$\mathbf{e}_i^{'}=\mathbf{Q}\mathbf{e}_i,$$
$$Q_{ij}=\cos\left(\mathbf{e}_i,\mathbf{e}_j^{'}\right).$$

The definition of the fourth-order stiffness tensor using transformation laws is expressed as follows:

$$C_{ijkl}^{'}=Q_{mi}Q_{nj}Q_{rk}Q_{sl}C_{mnrs}.$$

To transform the local stiffness matrix of each grain into the general stiffness matrix of the nanocrystal RVE, a symmetric Euler angle matrix is applied [27, 28]; the components of this matrix are as follows:

$$\begin{gathered} Q_{11}=-\sin\varphi\sin\omega-\cos\varphi\cos\omega\cos\theta, \\ Q_{12}=\sin\varphi\cos\omega-\cos\varphi\sin\omega\cos\theta, \\ Q_{13}=\cos\varphi\sin\theta, \\ Q_{21}=\cos\varphi\sin\omega-\sin\varphi\cos\omega\cos\theta, \\ Q_{22}=-\cos\varphi\cos\omega-\sin\varphi\sin\omega\cos\theta, \\ Q_{23}=\sin\varphi\sin\theta, \\ Q_{31}=\cos\omega\sin\theta, \\ Q_{32}=\sin\omega\sin\theta, \\ Q_{33}=\cos\theta. \end{gathered} \tag{6}$$

In Eq. (6), the variables φ, ω, and θ represent the angles corresponding to the orientation of each grain, and the elements of $\mathbf{Q}$ are the components of the symmetric Euler angle matrix.

2.2. RVE modeling

In this section, considering the existing assumptions, computational limitations, and, most importantly, the influence of the intermediate phase of the nanocrystal on its elastic properties, a suitable model is proposed for the nanocrystal RVE. In this research, the intermediate phase of the nanocrystal is considered as grain boundaries. Consequently, a crucial and vital parameter in modeling this issue is the ratio of the grain boundary thickness to the grain size. To determine this ratio, first, an acceptable range is extracted from other studies conducted in this field. Subsequently, utilizing the rule of mixtures and volumetric fraction of grain boundaries, the grain size and the grain boundary thickness are considered for modeling the RVE.

Experimental investigations and numerical simulations reveal that the change in the Young's modulus of nanocrystalline metals is directly influenced by the volumetric density of nanocrystals [3, 5, 15–17]. Moreover, these changes exhibit a meaningful relationship with both grain boundary thickness and grain size. The changes in the Young's modulus of nanocrystalline metals with grain cubic symmetry vary for larger grain sizes with a slight slope compared to smaller grain sizes. However, when the grain size decreases to less than 20 nm, the variations in the elastic modulus show a significant correlation with changes in grain size. A review of the research articles [3, 5, 15–17] indicates that the proposed distribution of grain size and grain boundary thickness suggests a volumetric density of grain boundaries in the RVE of the nanocrystal ranging from approximately 30 to 50 % [20–22, 29]. Consequently, the ratio of grain boundary thickness

to grain size is calculated to be around $1/10$ to $1/5$ using Eq. (7):

$$F = 1 - \left(1 - \frac{t}{D}\right)^3. \tag{7}$$

In Eq. (7), the variable t represents the thickness of the grain boundary, and D denotes the grain size. Notably, this equation was proposed in [20].

In this study, the rule of mixtures [30] is applied to microstructure problems for the modeling of the RVE. Grains are regarded as the matrix, while the grain boundaries are treated as the fibers. By applying the rule of mixtures to microstructure problems, the volume fraction of grains, V_g, and the volume fraction of grain boundaries, V_{gb}, are defined as follows:

$$V_g = \frac{v_g}{v_{\mathrm{RVE}}}, \quad V_{gb} = \frac{v_{gb}}{v_{\mathrm{RVE}}}.$$

It should be noted that in the above equation, v_{RVE} represents the total volume of the RVE of the nanocrystal. The relationship between V_g and V_{gb} is as follows:

$$V_g + V_{gb} = 1.$$

By employing the rule of mixtures and applying it to microstructure problems, Eq. (8) is derived. It should be noted that Eq. (8) provides the Young's modulus of the RVE as a weighted average of the moduli of the grain (E_g) and grain boundary (E_{gb}):

$$E_{\mathrm{RVE}} = E_{gb}V_{gb} + E_g(1 - V_{gb}), \tag{8}$$

where E_g is the bulk elastic modulus, i.e., the elastic modulus of a pure crystal (without grain boundary).

By dividing both sides of Eq. (8) by E_g, the equation is rewritten into the following form:

$$\frac{E_{\mathrm{RVE}}}{E_g} = \frac{E_{gb}}{E_g}V_{gb} + (1 - V_{gb}). \tag{9}$$

Given the ratio of the Young's modulus of the RVE to the bulk Young's modulus (i.e., E_{RVE}/E_g) for different grain sizes, and also considering the ratio of the Young's modulus of the grain boundaries to the bulk Young's modulus (i.e., E_{gb}/E_g), it is possible to calculate the volumetric fraction of grain boundaries, V_{gb}, and create the nanocrystal RVE. For this purpose, first, extract E_{RVE}/E_g and E_{gb}/E_g from the other conducted studies. Next, calculate the volumetric fraction of grain boundaries, V_{gb} through Eq. (9), and then determine the grain boundary thickness and grain size. These calculations are outlined in Eq. (10) for modeling a sample with a grain size of 6 nm. It should be noted that E_{RVE}/E_g and E_{gb}/E_g are extracted from [17]:

$$D = 6\,\mathrm{nm}, \quad \frac{E_{\mathrm{RVE}}}{E_g} = 0.7, \quad \frac{E_{gb}}{E_g} = 0.45 \rightarrow V_{gb} = 54\%. \tag{10}$$

For other samples with grain sizes of 9 and 12 nm, the same procedure is followed, and the results are summarized in Table 1.

Table 1. The grain size, grain boundary thickness, and grain boundary volume fraction extracted from [17]

D (nm)	t (nm)	V_{gb} (%)	E_{RVE}/E_g
6	2	54	0.7
9	2	42	0.75
12	2	34	0.8

A comparison of the values presented in Table 1 with the designated range for the ratio of grain boundary thickness to grain sizes (approximately 30 to 50%) demonstrates the validity and acceptability of the chosen ratio. All samples generated for various materials associated with their volumetric fractions are summarized in Table 2.

After determining the volumetric fractions of grains and grain boundaries (i.e., specifying the ratio of grain boundary thickness to grain size), the RVE of the nanocrystal is constructed using the method proposed in [15], which involves creating volumetric partitions on a cube with specified dimensions (Fig. 2).

As an example, a nanocrystal RVE is created using the aforementioned method, which involves creating volumetric partitions with a grain size of 10 nm and a grain boundary thickness of 1 nm in a cube with dimensions of $54 \times 54 \times 54$ nm (Fig 3). It is worth noting that the volumetric fraction of grain boundaries in this RVE is approximately 30%.

As a demonstration of the 3D model, several RVE are meticulously generated through the prescribed method and shown in Fig. 4. These RVEs feature grain sizes of 6, 9, and 12 nm from left to right, respectively, coupled with a constant grain boundary thickness of 1 nm (Fig. 4). It is evident from the accompanying figure below that, as grain sizes escalate while keeping grain boundary thickness constant, there is a reduction in the volumetric fraction of grain boundaries.

Table 2. The grain size, grain boundary thickness, and grain boundary volume fraction extracted from [3, 5, 15–17] for all case studies

Material	Cubic lattice	Sample No.	D (nm)	t (nm)	V_{gb} (%)
α-Fe	BCC	1	6	2	54
		2	9	2	42
		3	12	2	34
Cu	FCC	1	3.3	1	51
		2	5.2	1	40
		3	6.6	1	31
Al	FCC	1	6.7	2	51
		2	9	2	41
		3	11	2	36
Ta	BCC	1	3.3	1	51
		2	9	2	40
		3	6.6	1	31
Pd	FCC	1	3.3	1	51
		2	9	2	40
		3	6.6	1	31

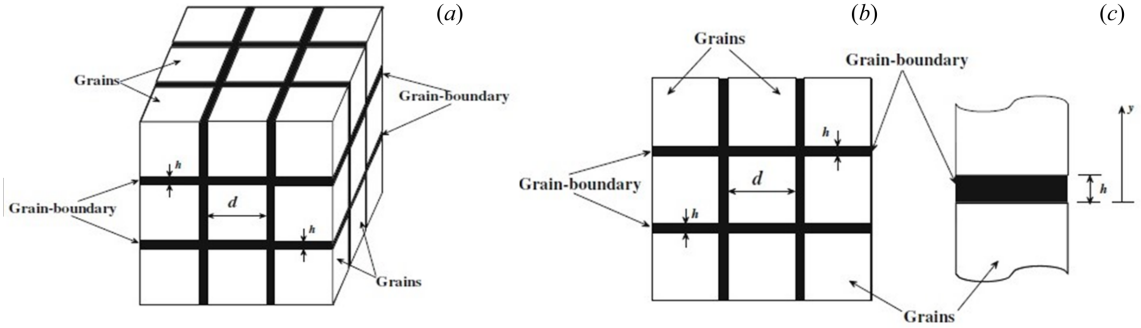

Fig. 2. The RVE created in [15] (*a*), view of the RVE front face (*b*), and enlarged fragment of the grain boundary (*c*)

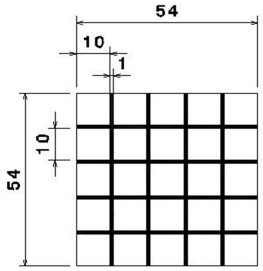

Fig. 3. The created RVE by applying the method presented in [15]

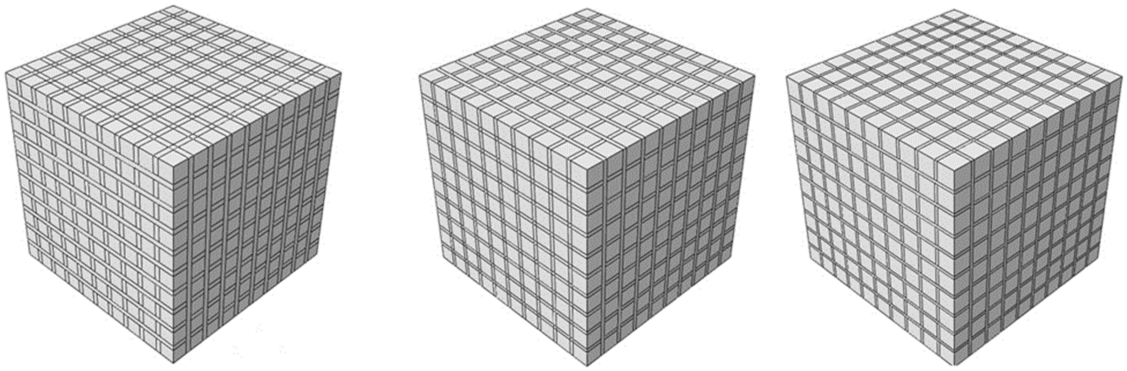

Fig. 4. 3D representation of RVEs with grain sizes 6, 9, and 12 nm from left to right, respectively

3. FE simulation

The nanocrystalline RVE is created through the partitioning method with 27 grains, a grain size of 10 nm, and a grain boundary thickness of 1 nm. Following the construction of the RVE, a behavioral model for the grains is established with cubic symmetry using the UMAT subroutine. To ensure the accuracy of the implementation, UMAT verification (includes simulations of uniaxial strain, uniaxial strain with limited rotation, and finite shear) is conducted. The behavior of grain boundaries is assumed to be elastically isotropic, and their elastic property (Young's modulus) is expressed as a coefficient of the entire RVE elastic properties. The coefficient considered for the grain boundary Young's modulus, denoted by symbol α, is referred to as the weakening coefficient. It is defined as the ratio of the Young's modulus of the grain boundary to that of the RVE, i.e., $\alpha = E_{gb}/E_{\mathrm{RVE}}$.

According to Eqs. (1) to (5) and assuming cubic symmetry of the grains, modeling the described behavior requires only the Young's modulus and Poisson's ratio of the isotropic material. Consequently, for the first simulation, the mechanical properties of copper metal (i.e., Young's modulus and Poisson's ratio) are applied and presented as follows:

Table 3. Cu mechanical properties [17]

Material	Module of elasticity (GPa)	Poisson's ratio
Copper Alloy C22000	115	0.33

After modeling and applying mechanical properties to all parts of the RVE, uniaxial tension is simulated and the RVE Young's modulus is calculated. For this purpose, the RVE is meshed in such a way that each grain is considered an element. By applying axial strain at a certain moment, the stress induced due to axial displacement is calculated for the RVE, Table 4. Finally, using the applied stress and strain, the RVE Young's modulus (E_{RVE}) is calculated. The boundary conditions for simulating uniaxial tension are as follows:

– Constrain the degrees of freedom of displacement in direction 1 for the lateral surface of the RVE;
– Constrain the degrees of freedom of displacement in direction 2 for the bottom surface of the RVE;
– Constrain the degrees of freedom of displacement in direction 3 for the front and back surfaces of the RVE;
– Apply displacement in the positive direction of axis 2 by an amount of 0.001 times the length of the cube edge on the upper surface of the RVE.

Table 4. The grain size, grain boundary thickness, grain boundary volumetric fraction, stress, applied deformation, and strain of the first simulation

D (nm)	t (nm)	V_{gb} (%)	Stress (MPa)	Deformation (nm)	Strain
10	1	27	20.22	0.032	0.001

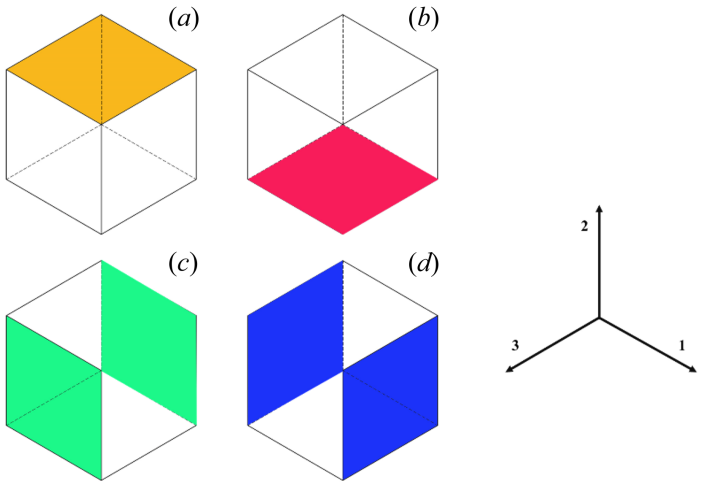

Fig. 5. The schematic of RVE different surfaces: top (a), bottom (b), back and front (c), lateral surfaces (d)

After simulating the first sample, it is necessary to evaluate the RVE in terms of the number of grains (n) to determine the appropriate number of grains for its convergence. For this purpose, three different samples with 3, 5, and 10 grains in each dimension, with equal grain size and equal grain boundary thickness, are created, and uniaxial tension is applied to calculate the Young's modulus of the RVE. The stress obtained for this simulation is tabulated separately in Table 5 for copper metal.

As shown in Table 5, as the number of grains increases, the changes become less significant, and when increased to 10 grains in each dimension (1000 in total), the relative changes are within 0.4%. Consequently, the FE simulation response

Table 5. The stress of the RVEs with varying numbers of grains

Sample No.	n	Stress (MPa)
1	27	19
2	125	20
3	729	20.14
4	1000	20.22

does not show significant variation, indicating model convergence and making it suitable as a reference model for all future simulations. Finally, 10 grains in each dimension are chosen (1000 in total), and the RVE is created.

Another point that needs to be evaluated is the convergence of the RVE based on the different grain orientations. For this purpose, it is necessary to simulate the RVE with three different sets of grain orientations, and the results of these simulations should be compared with each other. The convergence of the responses indicates that the created RVE is independent of the grain orientations.

In Table 6, σ_1, σ_2, and σ_3 denote the tensile stress resulting from the first, second, and third set of grain orientations, respectively. As observed in Table 6, the variations in stress based on changes in the orientations of the RVE are negligible. Consequently, it can be concluded that the RVE is independent of the grain orientations.

Table 6. The grain size, grain boundary thickness, number of grains, and stress in all grain orientations

D (nm)	t (nm)	n	σ_1 (MPa)	σ_2 (MPa)	σ_3 (MPa)
10	1	1000	20.2221	20.2222	20.2225

To ensure the isotropy of the RVE, uniaxial tension is simulated in all three directions: 1, 2, and 3. If the obtained elastic modulus values are consistent across all directions, it ensures the isotropy of the RVE. Notably, the boundary conditions for simulating tension in directions 2 and 3 are identical to those in direction 1. The summarized results of these simulations are presented in Table 7.

Table 7. The grain size, grain boundary thickness, grain boundary volumetric fraction, and the Young's modulus in all three directions

D (nm)	t (nm)	V_{gb} (%)	E_1 (GPa)	E_2 (GPa)	E_3 (GPa)
12	2	34	145.045	145.042	145.047

In Table 7, E_1, E_2, and E_3 represent the Young's modulus in directions 1, 2, and 3, respectively. From the results presented in Table 7, it is evident that the variations of the RVE Young's modulus in all directions are negligible; hence, the isotropy of the RVE is ensured.

It should be noted that the values of the Young's modulus of Copper Alloy C22000 calculated from the above simulations (Table 7) differ from those extracted from [17], Table 3. This difference is due to the fact that the correct weakening coefficient has not yet been determined in the performed simulations.

4. Results and discussion

The final simulation is conducted on 5 different metal samples with varying BCC and FCC structures, Table 2. For each metal, three samples are created with specific grain sizes and grain boundary thicknesses. For each sample, 8 uniaxial tensile simulations with different weakening coefficients are performed. The Young's modulus of the RVE is calculated from the applied stress and the strain imposed on the RVE. Subsequently, the results obtained from applying the FEM to the created models are discussed in Fig. 6.

Figure 6 demonstrates the Young's modulus of the RVE based on variations in the weakening coefficient for the metals under investigation. The horizontal axis of this figure represents the weakening coefficient, while the vertical axis represents the Young's modulus. As observed in this figure, with an increase in the weakening coefficient, increasing in the Young's modulus of the grain boundaries, the Young's modulus of the RVE nanocrystal also increases. This figure demonstrates the effect of the weakening coefficient of grain boundaries with constant thickness on the Young's modulus of the RVE. Additionally, the FE simulations conducted for each case study resulted in three values for the weakening coefficient. By calculating the average of these values, the final weakening coefficient for each case is determined, Table 8.

The validation and verification of the obtained weakening coefficient are ensured by comparing the calculated Young's modulus of the RVE through the FEM, with the results of experimental tests and MD simulations from other studies [3, 5, 15–17]. For better and easier comparison, these values are plotted together in the same figure based on variations in the volumetric fraction of grain boundaries (Fig. 7).

As observed in Fig. 7, the results obtained from FE simulations exhibit a good agreement with the results extracted from other studies for all samples. This suitable agreement validates the obtained weakening coefficient. Moreover, from

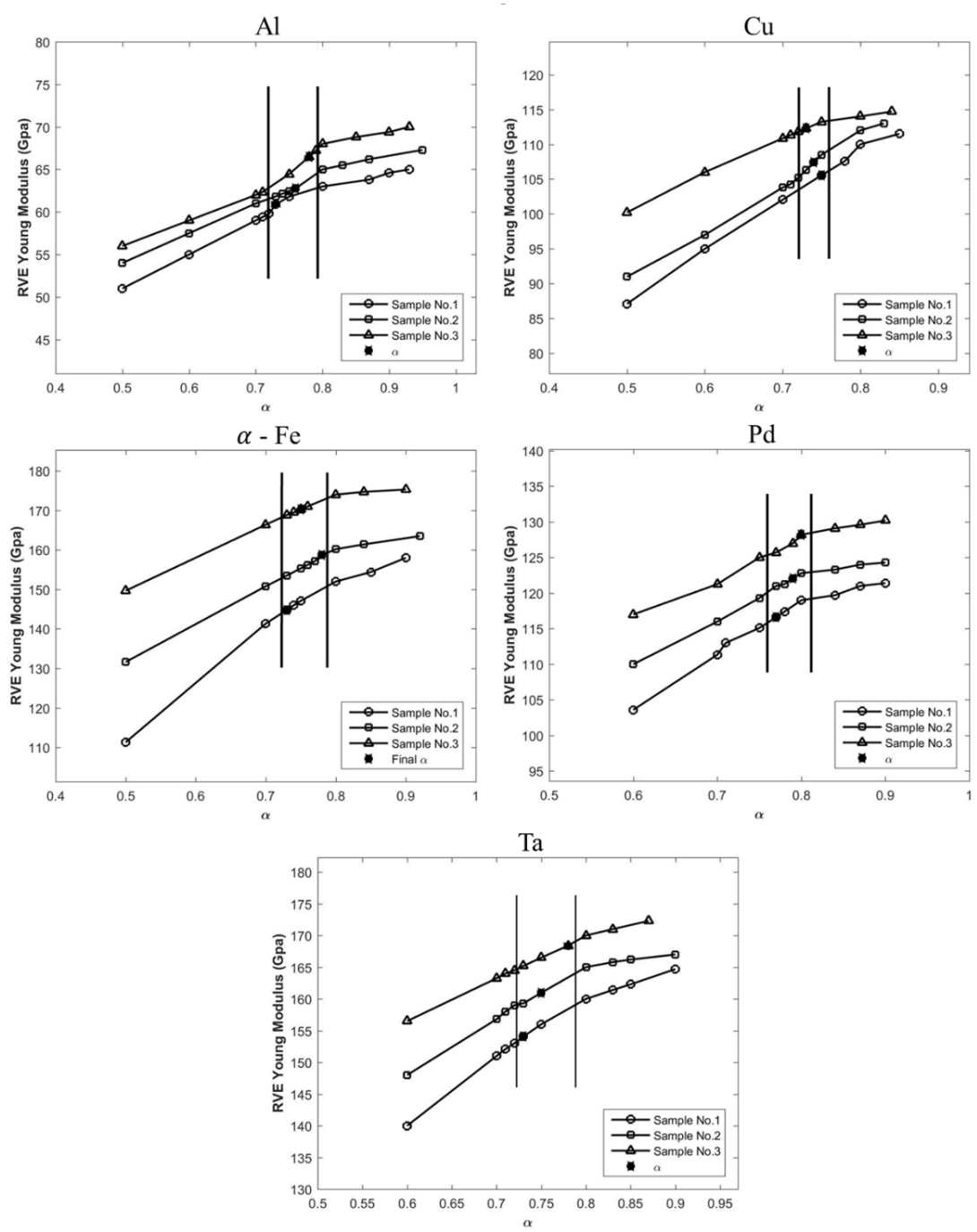

Fig. 6. Changes in the Young's modulus of RVEs based on variations in the weakening coefficient for different materials

Table 8. The ultimate weakening coefficient specified for each metal

Sample No.	Metal	Cubic structure	Weakening coefficient
1	α-Fe	BCC	0.75
2	Cu	FCC	0.74
3	Al	FCC	0.76
4	Ta	BCC	0.75
5	Pd	FCC	0.79

this figure, it can be seen that an increase in the volumetric fraction of grain boundaries, leading to a higher influence of the nanocrystal's intermediate phase (i.e., grain boundaries), results in a decreased Young's modulus. It is worth noting that this observation is consistent with findings from other studies conducted in this field [3, 5, 15–17]. Another outcome

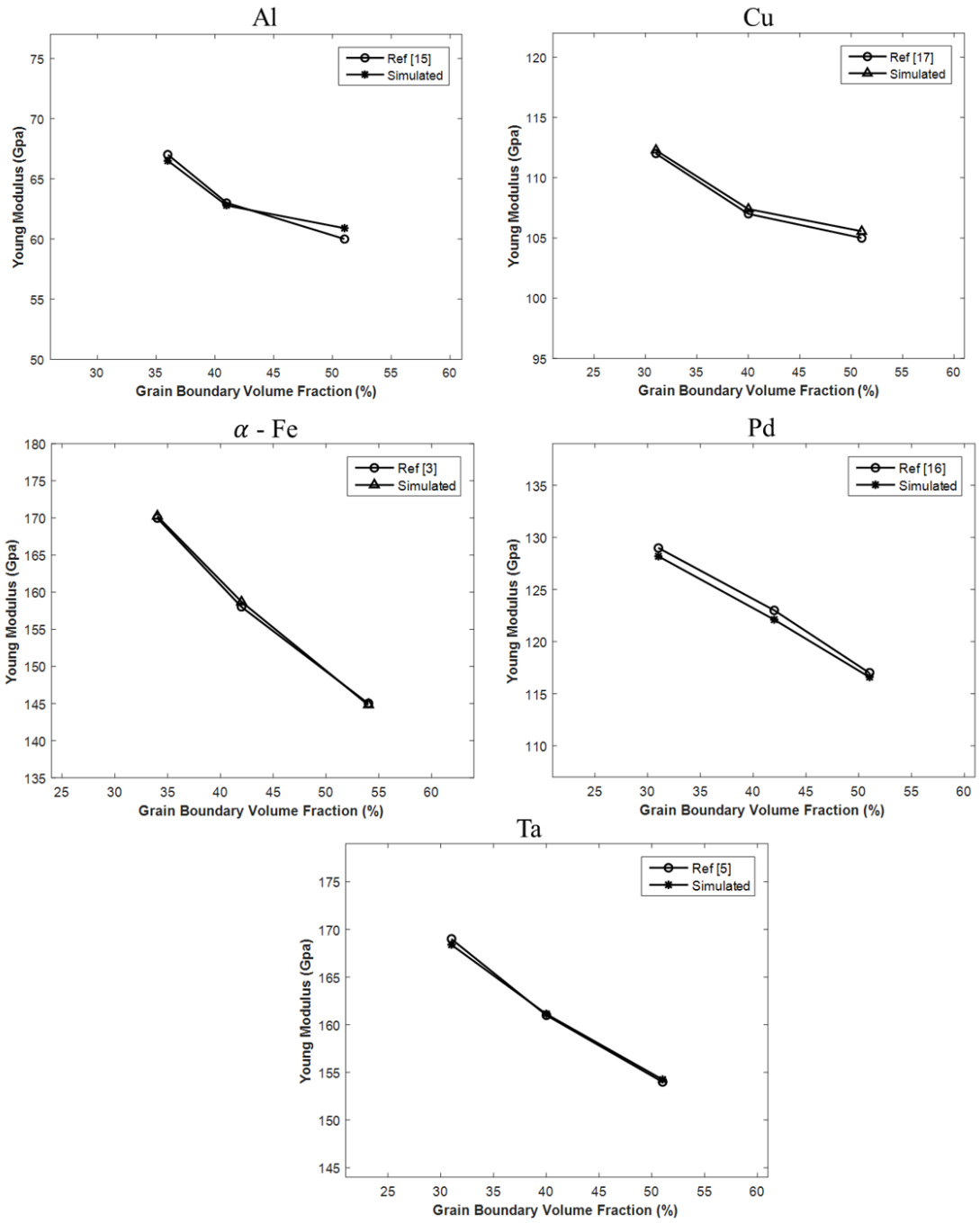

Fig. 7. Changes in the Young's modulus of RVEs based on grain boundary volumetric fraction for different materials

observed from this figure is the effect of the volume fraction of grain boundaries on the Young's modulus of the RVE; the Young's modulus of the RVE changes exponentially with variations in the volume fraction of grain boundaries.

After validating the conducted simulations and the obtained weakening coefficient for all case studies, the final weakening coefficient for each metal is calculated through averaging the provided values, Table 8.

Using the calculated weakening coefficient for different metals with varying crystal structures, it is possible to determine and present the range of variation for the weakening coefficient in nanocrystalline metals; the calculated weakening coefficient falls within the range of 0.74 to 0.79. The minimal variance demonstrated in this range allows for the determination of an average weakening coefficient of 0.76 for crystalline metals.

5. Conclusion

Based on the significant influence of grain boundaries as a key component of nanocrystalline metals on their overall elasticity, the primary objective of this research was to model and calculate the elasticity of grain boundaries in nanocrystalline metals. For this purpose, five nanocrystalline metals with different crystal structures were chosen, and their grain boundary elasticities were calculated. To calculate the grain boundary elasticity, first, an RVE was created based on

parameters such as the grain boundary thickness to grain size ratio and the volumetric fraction of grain boundaries. Next, for each RVE, a constant grain boundary thickness and variable grain sizes were considered, resulting in different grain boundary volumetric fractions; this procedure was performed for all sample metals. Then, the behavior of each part of this RVE, namely, the cubic symmetry for grains and the elastically isotropic for grain boundaries, was simulated by applying a desired weakening coefficient of elasticity from the macroscopic elastic modulus of the sample metal. Then, uniaxial tensile tests were simulated to calculate the Young's modulus of the RVEs. For each of them, eight simulations were carried out to achieve the target Young's modulus, extracted from experimental studies, and the weakening coefficient for the RVE was computed. Finally, the final weakening coefficient for each metal was determined by averaging the provided values. The main conclusions are concise as follows:

– the elasticity of grain boundaries in nanocrystalline metals was proposed as a coefficient of the overall elasticity of nanocrystals. This coefficient was introduced as a weakening coefficient and was identified within the range of 0.74 to 0.79. Due to the slight range of variations in the proposed weakening coefficient, an averaging process yielded a value of 0.76 for this coefficient in nanocrystalline metals.

– at a constant grain boundary thickness, the Young's modulus of the RVE increases with the grain size; this trend aligns with other research conducted in this field.

– an increase in the weakening coefficient leads to an increase in the Young's modulus of grain boundaries; consequently, the overall Young's modulus of nanocrystals increases.

– a increase in the volume fraction of grain boundaries leads to a reduction in the overall Young's modulus of nanocrystals. This trend arises from the increased influence of grain boundaries due to the rising volume fraction of grain boundaries.

– the volume fraction of grain boundaries significantly affects the overall Young's modulus of nanocrystals; this effect has an exponential form.

– the validity of the Young's modulus calculated using the proposed method in this study was verified by observing the good agreement between the Young's modulus obtained in this research and that presented in other studies conducted in this field.

References

1. *Forrest R.M.*, *Lazar E.A.*, *Goel S.*, *Bean J.J.* Quantifying the differences in properties between polycrystals containing planar and curved grain boundaries. Nanofabrication. 2022. Vol. 7. P. 11–23. DOI: 10.37819/nanofab.007.250
2. *Valat-Villain P.*, *Durinck J.*, *Renault P.O.* Grain Size Dependence of Elastic Moduli in Nanocrystalline Tungsten. Journal of Nanomaterials. 2017. Vol. 2017. DOI: 10.1155/2017/3620910
3. *Latapie A.*, *Farkas D.* Effect of grain size on the elastic properties of nanocrystalline α-iron. Scripta Materialia. 2003. Vol. 48, no. 5. P. 611–615. DOI: 10.1016/S1359-6462(02)00467-0
4. *Wang N.*, *Wang Z.*, *Aust K.T.*, *Erb U.* Effect of grain size on mechanical properties of nanocrystalline materials. Acta Metallurgica et Materialia. 1995. Vol. 43, no. 2. P. 519–528. DOI: 10.1016/0956-7151(94)00253-E
5. *Pan Z.*, *Li Y.*, *Wei Q.* Tensile properties of nanocrystalline tantalum from molecular dynamics simulations. Acta Materialia. 2008. Vol. 56, no. 14. P. 3470–3480. DOI: 10.1016/j.actamat.2008.03.025
6. *Xu W.*, *Dávila L.P.* Size dependence of elastic mechanical properties of nanocrystalline aluminum. Materials Science and Engineering: A. 2017. Vol. 692. P. 90–94. DOI: 10.1016/j.msea.2017.03.065
7. *Zheng L.*, *Xu T.-D.* Method for determining the elastic modulus at grain boundaries for polycrystalline materials. Materials Science and Technology. 2004. Vol. 20, no. 5. P. 605–609. DOI: 10.1179/026708304225012017
8. *Zhu L.*, *Zheng X.* Influence of interface energy and grain boundary on the elastic modulus of nanocrystalline materials. Acta Mechanica. 2010. Vol. 213, no. 3/4. P. 223–234. DOI: 10.1007/s00707-009-0263-3
9. *Lai W.M.*, *Rubin D.*, *Krempl E.* Introduction to continuum mechanics. Butterworth-Heinemann, 2009
10. *Diana V.* Anisotropic Continuum-Molecular Models: A Unified Framework Based on Pair Potentials for Elasticity, Fracture and Diffusion-Type Problems. Archives of Computational Methods in Engineering. 2023. Vol. 30, no. 2. P. 1305–1344. DOI: 10.1007/s11831-022-09846-0
11. *Yeheskel O.*, *Chaim R.*, *Shen Z.*, *Nygren M.* Elastic moduli of grain boundaries in nanocrystalline MgO ceramics. Journal of Materials Research. 2005. Vol. 20, no. 3. P. 719–725. DOI: 10.1557/JMR.2005.0094
12. *Kim T.-Y.*, *Dolbow J.E.*, *Fried E.* Numerical study of the grain-size dependent Young's modulus and Poisson's ratio of bulk nanocrystalline materials. International Journal of Solids and Structures. 2012. Vol. 49, no. 26. P. 3942–3952. DOI: 10.1016/j.ijsolstr.2012.08.023
13. *Borokinni A.S.*, *Akinola A.P.*, *Layeni O.P.*, *Fadodun O.O.* A new strain-gradient theory for an isotropic plastically deformed polycrystalline solid body. Mathematics and Mechanics of Solids. 2018. Vol. 23, no. 9. P. 1333–1344. DOI: 10.1177/1081286517720842
14. *Gurtin M.E.*, *Murdoch A.I.* A continuum theory of elastic material surfaces. Archive for Rational Mechanics and Analysis. 1975. Vol. 57. P. 291–323. DOI: 10.1007/BF00261375
15. *Zhou J.*, *Li Y.*, *Zhu R.*, *Zhang Z.* The grain size and porosity dependent elastic moduli and yield strength of nanocrystalline ceramics. Materials Science and Engineering: A. 2007. Vol. 445/446. P. 717–724. DOI: 10.1016/j.msea.2006.10.005
16. *Sanders P.G.*, *Eastman J.A.*, *Weertman J.R.* Elastic and tensile behavior of nanocrystalline copper and palladium. Acta Materialia. 1997. Vol. 45, no. 10. P. 4019–4025. DOI: 10.1016/S1359-6454(97)00092-X
17. *Schiøtz J.*, *Di Tolla F.D.*, *Jacobsen K.W.* Softening of nanocrystalline metals at very small grain sizes. Nature. 1998. Vol. 391, no. 6667. P. 561–563. DOI: 10.1038/35328

ISSN: 1999-6691, e-ISSN: 2782-3709 DOI: http://doi.org/10.7242/1999-6691/2025.18.2.14

18. *Suryanarayana C.*, *Froes F.H.* The structure and mechanical properties of metallic nanocrystals. Metallurgical Transactions A. 1992. Vol. 23. P. 1071–1081. DOI: 10.1007/BF02665039

19. *Korn D.*, *Morsch A.*, *Birringer R.*, *Arnold W.*, *Gleiter H.* Measurements of the elastic constants, the specific heat and the entropy of grain boundaries by means of ultra-fine grained materials. Le Journal de Physique Colloques. Vol. 49. 1988. P. 769–779. DOI: 10.1051/jphyscol:1988596

20. *Trelewicz J.R.*, *Schuh C.A.* Grain boundary segregation and thermodynamically stable binary nanocrystalline alloys. Physical Review B. 2009. Vol. 79, no. 9. P. 094112. DOI: 10.1103/PhysRevB.79.094112

21. *Wei Y.*, *Su C.*, *Anand L.* A computational study of the mechanical behavior of nanocrystalline fcc metals. Acta Materialia. 2006. Vol. 54, no. 12. P. 3177–3190. DOI: 10.1016/j.actamat.2006.03.007

22. *Shimokawa T.*, *Nakatani A.*, *Kitagawa H.* Grain-size dependence of the relationship between intergranular and intragranular deformation of nanocrystalline Al by molecular dynamics simulations. Physical Review B. 2005. Vol. 71, no. 22. P. 224110. DOI: 10.1103/PhysRevB.71.224110

23. *Kuleyev I.I.*, *Kuleyev I.G.* Dynamic Properties and Focusing of Phonons in Metallic and Dielectric Crystals of Cubic Symmetry. Review 1. Physics of Metals and Metallography. 2023. Vol. 124, S1. P. S2–S31. DOI: 10.1134/S0031918X23601993

24. *Lord E.A.*, *Mackay A.L.* Periodic minimal surfaces of cubic symmetry. Current Science. 2003. P. 346–362. DOI: 10.2307/24108665

25. *Hürlimann T.* Index notation in mathematics and modelling language LPL: theory and exercices. Fribourg, Switzerland: Department of Informatics University of Fribourg, 2007

26. *Povey R.G.* Voigt transforms. 2023. URL: https://rhyspovey.com/science/voigt.pdf

27. *Ben-Ari M.* A tutorial on euler angles and quaternions. Israel, 2014. URL: https://raw.githubusercontent.com/motib/mathematics/master/quaternions/quaternion-tutorial.pdf

28. *Diebel J.* Representing attitude: Euler angles, unit quaternions, and rotation vectors. Matrix. 2006. Vol. 58, no. 15/16. P. 1–35.

29. *Hahn H.*, *Mondal P.*, *Padmanabhan K.A.* Plastic deformation of nanocrystalline materials. Nanostructured Materials. 1997. Vol. 9, no. 1–8. P. 603–606. DOI: 10.1016/S0965-9773(97)00135-9

30. *Shunmugesh K.*, *Raphel A.*, *Unnikrishnan T.G.*, *Akhil K.T.* Finite element modelling of carbon fiber reinforced with vespel and honey-comb structure. Materials Today: Proceedings. 2023. Vol. 72. P. 2163–2168. DOI: 10.1016/j.matpr.2022.08.301

Authors' Details:

Alireza Talakesh (corr.), Department of Mechanical Engineering, University of Isfahan, Isfahan, 81746-73441, Iran; e-mail: a.talakesh@eng.ui.ac.ir; ORCID: 0009-0009-5513-4835

Amir Torabi, Department of Mechanical Engineering, Ferdowsi University of Mashhad, Mashhad, 91775-1111, Iran; ORCID: 0000-0003-4727-698X

Научная статья

Конечно-элементное моделирование пониженной упругости границ зерен в нанокристаллических металлах

А. Талакеш [1], ***А. Тораби*** [2]

[1] *Исфаханский университет, Исфахан, Иран*
[2] *Мешхедский университет имени Фирдоуси, Мешхед, Иран*

Нанокристаллические металлы состоят из двух различных фаз: кристаллической фазы, а именно зерен, и межкристаллической фазы, которая включает границы зерен, тройные соединения и четверные узлы. Ослабление упругости в межкристаллитной фазе нанокристаллических металлов, особенно на границах зерен, приводит к снижению общего модуля упругости. Следовательно, изучение упругих свойств и расчет упругости границ зерен имеет решающее значение для понимания нанокристаллических металлов. Целью данного исследования является моделирование упругости границ зерен в нанокристаллических металлах и ее расчет. Для этого рассмотрено пять образцов металла с различной кристаллической структурой. Для каждого образца моделируются три представительных объемных элемента с различными размерами зерен и постоянной толщиной границ зерен. Предполагается, что кристаллическая фаза упругая с кубической симметрией, в то время как границы зерен являются упругоизотропными. Затем с помощью конечно-элементного анализа моделируется одноосное растяжение для расчета модуля Юнга объемного элемента. В результате этого получается коэффициент ослабления границ зерен. Чтобы проверить достоверность этого коэффициента, модуль Юнга моделируемого представительного объемного элемента сравнивается с модулем Юнга, полученным моделированием на основе молекулярной динамики и в экспериментах, описанных в литературе.

Ключевые слова: зерно, граница раздела зерен, нанокристаллические металлы, представительные объемные элементы, коэффициент ослабления, модуль Юнга

Получение: 30.05.2024 / *Публикация онлайн*: 30.07.2025 УДК 539.3+620.172.2